JCTC Journal of Chemical Theory and Computation

pubs.acs.org/JCTC Letter

Generalized Born Implicit Solvent Models Do Not Reproduce Secondary Structures of *De Novo* Designed Glu/Lys Peptides

Eric J. M. Lang,* Emily G. Baker, Derek N. Woolfson, and Adrian J. Mulholland*

Cite This: *J. Chem. Theory Comput.* 2022, 18, 4070−4076 Read Online

ACCESS | Metrics & More | Article Recommendations | Supporting Information

ABSTRACT: We test a range of standard generalized Born (GB) models and protein force fields for a set of five experimentally characterized, designed peptides comprising alternating blocks of glutamate and lysine, which have been shown to differ significantly in α-helical content. Sixty-five combinations of force fields and GB models are evaluated in >800 μs of molecular dynamics simulations. GB models generally do not reproduce the experimentally observed α-helical content, and none perform well for all five peptides. These results illustrate that these models are not usefully predictive in this context. These peptides provide a useful test set for simulation methods.

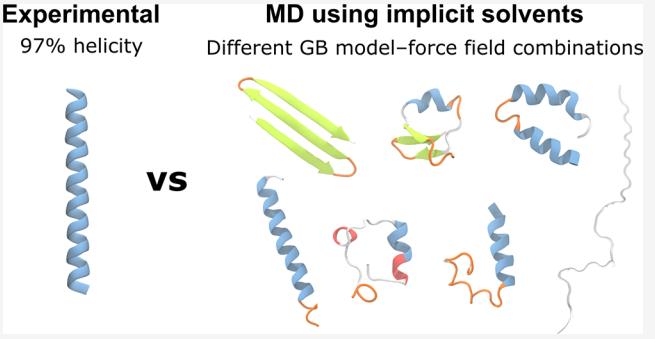

Molecular dynamics (MD) simulations have demonstrated their worth and are now an established technique, complementing experiment, in structural biology.[1] MD simulations are also contributing increasingly to *de novo* protein design and also have a role in protein structure prediction. In design, typically many model structures must be evaluated, making MD simulations computationally expensive. MD simulations of designed proteins are often currently limited to short backbone-restrained simulations to improve side-chain packing.[2,3] Protein design protocols could potentially benefit from incorporating more extensive unrestrained MD simulations routinely to test the stabilities of designed structures, to help design dynamical/conformational properties, and to improve understanding of sequence-to-structure/function relationships.[4−6] An attractive, practical solution is to use implicit solvent models. These typically aim to include dielectric shielding and other effects of aqueous solvation, while avoiding the computational cost of explicit representation of large numbers of water molecules.[7,8]

Although explicit solvent simulations are in general more accurate, currently they are too computationally expensive for routine use in protein design pipelines that generate many constructs. Simulations using implicit solvent—such as those based on generalized Born (GB) models—are faster and easier to set up and analyze. Moreover, because protein dynamics are not damped by solvent viscosity, conformational space sampling is accelerated.[9,10] Although GB models have been used successfully in many studies, they have well-known limitations: e.g., different GB model−force field combinations can to lead to very different results, with many combinations unable to reproduce native folds.[11−13] Nonetheless, recent work suggests that the latest GB models and force fields have improved accuracy and reproduce the observed structures for a test set of small proteins, without the need to include nonelectrostatic terms such as effects of solvent accessible surface area.[14]

To test GB models, we simulate here a systematic series of *de novo* peptides, which we designed and experimentally characterized previously to explore electrostatic interactions in single α helices.[15] They comprise blocks of negatively charged glutamate (Glu, E) and positively charged lysine (Lys, K) residues in sequences of the type $(E_xK_x)_n$ or $(K_xE_x)_n$, Table 1. Rational changes in lengths and sequences of the charged blocks result in strikingly different experimentally observed α-helical contents. Our aim was to identify a useful simulation model to assist protein design.

Interest in such peptides is not limited to *de novo* design: they are also models for naturally occurring ER/K motifs, i.e., alternating repeats of Glu and Lys or arginine (Arg, R).[16] Such motifs are found in all kingdoms of life and in ≈0.2−0.5% of all proteins and form stable α-helical structures in the absence of tertiary interactions.[17−19] As such, they are also called single α-helical domains (SAHs). Notably, MD simulations of these domains using different force fields and with explicit TIP3P water models have been able to reproduce the experimental helicities.[16,20−22]

Received: November 19, 2021
Published: June 10, 2022

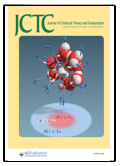

Table 1. *De Novo* Peptides[a] Used for Testing Different Force Field–GB Model Combinations

Peptide[a]	Sequence[b]	α helicity using CD MRE_{222} (%)[c]	α helicity using BeStSel (%)[d]
$A_4(K_4E_4)_1A_4(K_4E_4)_1A_4$	Ac–GAAAAKKKKEEEEAAAAKKKKEEEEAAAAGW–NH_2	97	77
$(E_4K_4)_2$	Ac–GEEEEKKKKEEEEKKKKGW–NH_2	65	61
$(K_4E_4)_2$	Ac–GKKKKEEEEKKKKEEEEGW–NH_2	22	19
$(E_4K_4)_3$	Ac–GEEEEKKKKEEEEKKKKEEEEKKKKGW–NH_2	74	63
$(K_4E_4)_3$	Ac–GKKKKEEEEKKKKEEEEKKKKEEEEGW–NH_2	62	54

[a]Previously experimentally characterized by Baker et al.[15] [b]Peptide sequences *N*- and *C*-terminally capped with acetyl (Ac) and amide (NH_2) groups, respectively. Lys residues are colored blue, and Glu residues are colored red. [c]Experimentally determined α helicities from circular dichroism (CD) spectroscopy measurements (5 °C in phosphate-buffered saline, pH 7.4) of mean residue ellipticity (MRE) at 222 nm.[15] α Helicities were determined by BeStSel[24] analysis of the CD spectra in the range of 200–250 nm.

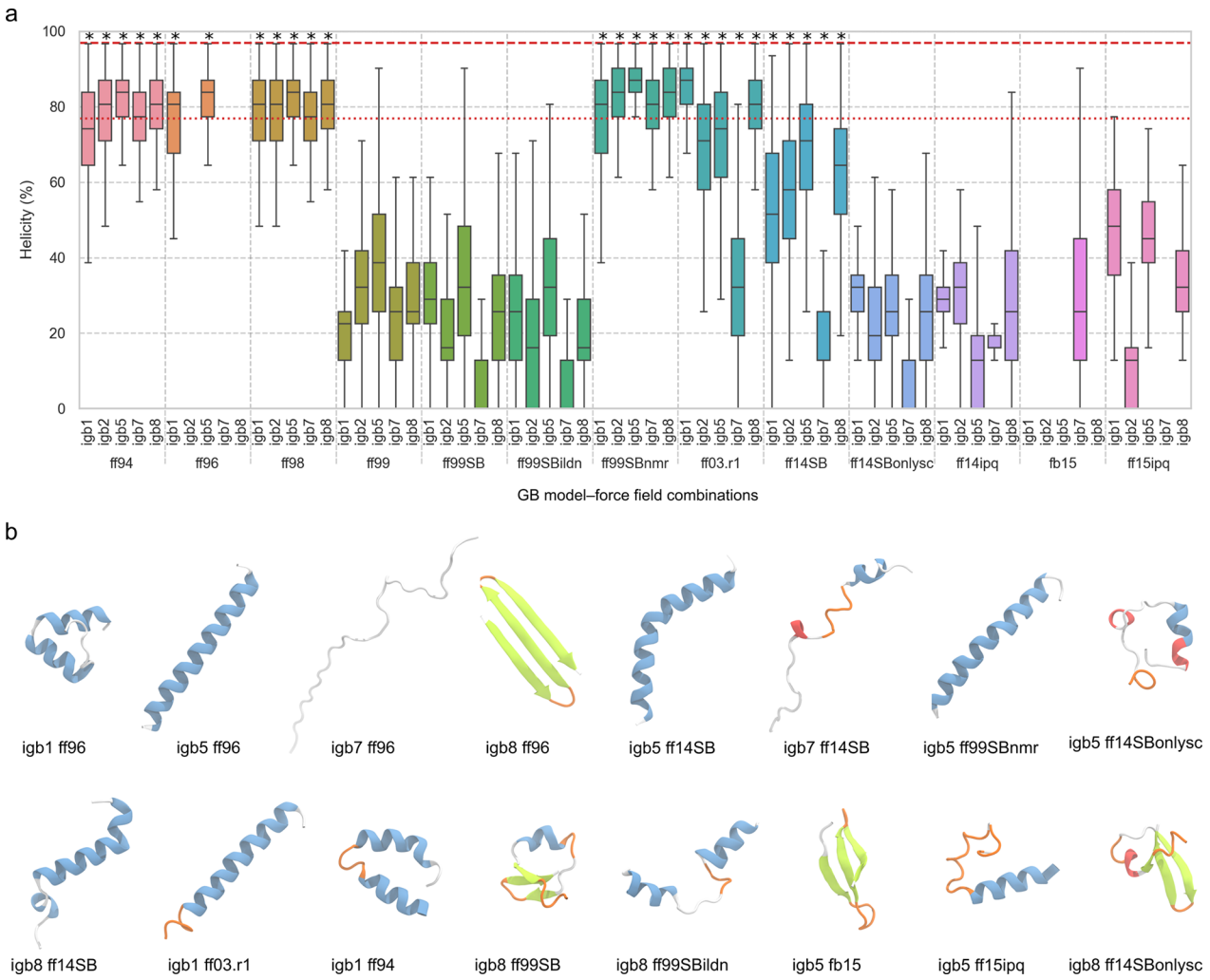

Figure 1. Predicted α helicities and final structures from MD simulations of $A_4(K_4E_4)_1A_4(K_4E_4)_1A_4$ using 65 GB model–force field combinations. (**a**) Percentage helicity of $A_4(K_4E_4)_1A_4(K_4E_4)_1A_4$ calculated with DSSP[43] for the MD trajectories generated for all 65 combinations. The results are presented as boxplots with the boxes indicating the first quartile, the median, and the third quartile of the sample. The whiskers indicate 1.5 times the interquartile range. Gaps correspond to combinations for which the percentage α helicity is negligible. For each combination, 5750 frames were analyzed. Each force field is represented with a different color. The red dashed line represents the experimental helicity using mean residue ellipticity (MRE) at 222 nm,[15] while the red dotted line corresponds to the helicity obtained with BeStSel by analyzing the CD spectra in the range of 200–250 nm. Asterisks indicate the GB model–force field combinations selected for further testing (Figure 2). (**b**) Backbone structures of $A_4(K_4E_4)_1A_4(K_4E_4)_1A_4$ from selected GB model–force field combinations after 6 μs of MD. The peptides are colored by structure: α helix, blue; extended β-strand and β-bridge, green; π-helix, red; 3_{10} helix, purple; turn, orange; coil, white.

Here, we simulate five *de novo* sequences (Table 1) using five different GB models and 13 different force fields, using the AMBER16 biomolecular simulation program.[23]

We tested the five GB models available in AMBER16: the Hawkins, Cramer, Truhlar model[25] (igb1); the Onufriev, Bashford, Case model[26,27] (igb2) and its modified version[27] (igb5); and the GBn model by Mongan, Simmerling, McCammon, Case, and Onufriev[28] (igb7) and its modified version by Nguyen, Roe, and Simmerling[29] (igb8). In combination with these, 13 AMBER force fields were tested:

https://doi.org/10.1021/acs.jctc.1c01172
J. Chem. Theory Comput. 2022, 18, 4070–4076

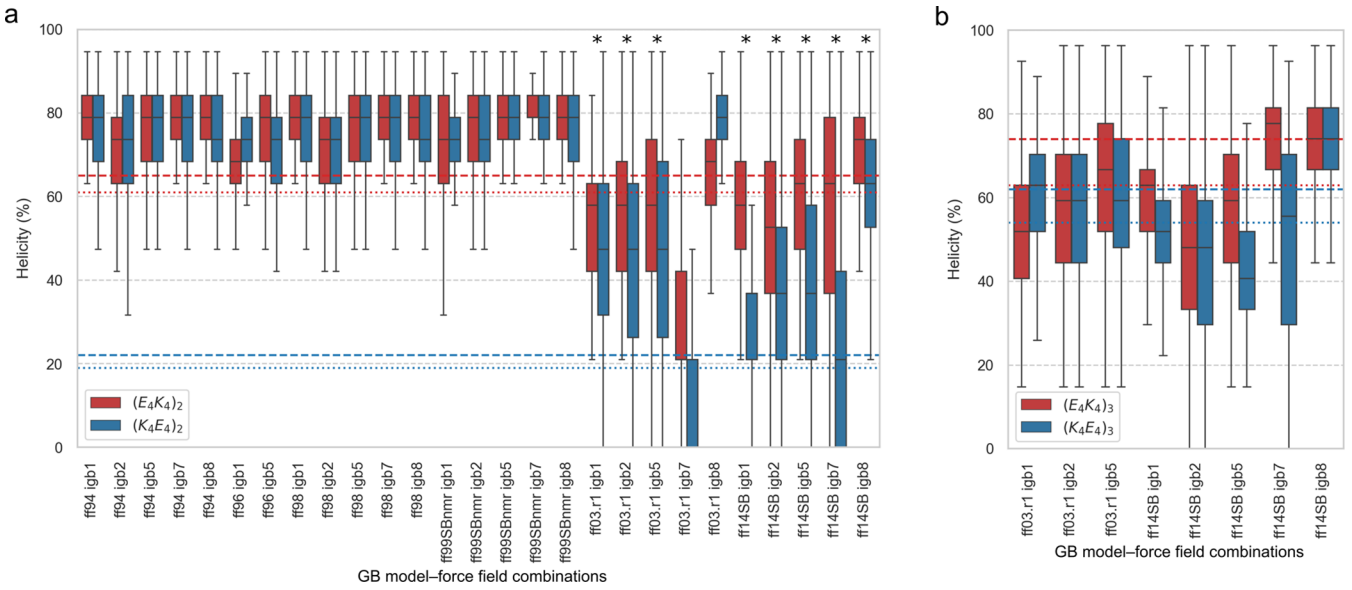

Figure 2. DSSP[43] calculated α helicities of $(E_4K_4)_n$ and $(K_4E_4)_n$ peptides, where n = 2, 3. (**a**) Percentage α helicities of $(E_4K_4)_2$ (red) and $(K_4E_4)_2$ (blue) for the MD trajectories generated from 27 GB model−force field combinations. Asterisks indicate the combinations selected for MD simulations of longer peptide variants $(E_4K_4)_3$ and $(K_4E_4)_3$. (**b**) Percentage α helicities of $(E_4K_4)_3$ (red) and $(K_4E_4)_3$ (blue) for the MD trajectories from eight GB model−force field combinations. (**a** and **b**) The results are presented as boxplots as in Figure 1. The dashed lines show the experimentally measured helicities for each $(E_4K_4)_n$ peptide in red and each $(K_4E_4)_n$ peptide in blue using mean residue ellipticity (MRE) at 222 nm,[15] and the dotted lines correspond to the helicity obtained with BeStSel by analyzing the CD spectra in the range of 200−250 nm.

ff94,[30] ff96,[31] ff98,[32] ff99,[33] ff99SB,[34] ff99SBildn,[35] ff99SBnmr,[36] ff03.r1,[37] ff14SB,[38] ff14SBonlysc,[38] ff14ipq,[39] fb15,[40] and ff15ipq,[41] i.e., 65 GB model/force field combinations in total.

The choice of GB models and AMBER was made for the following reasons. First, these GB models have been implemented in most of the major biomolecular MD packages: all five in AMBER and OpenMM; igb1, igb2, and igb5 in GROMACS; and igb2 in NAMD. Second, the GPU MD engine pmemd.cuda[42] within AMBER is fast and ideal for rapid testing of multiple GB model−force field combinations.

Conditions from the experiments[15] were replicated as closely as possible: the peptides were *N*-terminally acetylated and *C*-terminally amidated; the simulations were run at 278.15 K; and the ionic concentration was set to 0.137 mol/L to mimic that of phosphate buffered saline (pH 7.4). Glu and Lys side chains were treated as fully ionized, i.e., negatively and positively charged, respectively, yielding neutral peptides. Initially, single 6 μs simulations were run for each GB model−force field combination, with some systems repeated four times to test reproducibility (see below). All simulations used the same minimization, heating, and equilibration protocols (see Methods in the Supporting Information), starting from a fully α-helical structure of each peptide. The first 250 ns were discarded as further equilibration, yielding 5.75 μs of production MD for each. 5750 frames (saved every 1 ns) were analyzed for each peptide.

We began with peptide $A_4(K_4E_4)_1A_4(K_4E_4)_1A_4$ because this is the most helical experimentally (Table 1). The helicities and structures from the MD simulations of this peptide for each GB model−force field combination are shown in Figure 1.

None of the GB model−force field combinations gave fully helical structures throughout the trajectories (Figure 1a). Moreover, a disconcertingly large array of conformations was observed (Figure 1b) with some structures being completely unfolded and others that did not maintain a stable secondary structure for more than a few nanoseconds or were completely reconfigured into β sheets (Movies S1 and S2). There is no experimental evidence (from circular dichroism or NMR spectroscopy) that the $A_4(K_4E_4)_1A_4(K_4E_4)_1A_4$ peptide accesses these states in these conditions.[15]

The best performing combination was igb5 with ff99SBnmr (Movie S1), with a median helicity of ≈87% and an interquartile range of less than 10% over the course of the simulation. The slight loss of helicity was due to the unfolding of the terminal residues at both ends. Irrespective of the implicit solvent model, ff99SBnmr performed reasonably well for $A_4(K_4E_4)_1A_4(K_4E_4)_1A_4$, in contrast to the related ff99SB, ff99SBildn, and ff99 force fields (median α helicity < 50%). The older force fields ff94 and ff98 yielded a median helicity above 75% and an interquartile range below 20%, regardless of the GB model used, and were among the best force fields at capturing the helical structure of this peptide.

The most recent GB model−force field combination, igb8 with ff14SBonlysc, which is recommended by the AMBER developers,[14,29] did not maintain the starting α helix (Figure 1b, bottom right) or even a stable overall secondary structure (Movie S1). Changing the GB model did not significantly modify the outcome with this force field. Surprisingly, the ff14SB force field, which was parametrized for use with the explicit TIP3P water model, led to a higher simulated α helicity than ff14SBonlysc for each GB model, Figure 1 and Movie S1. Unsurprisingly, force fields ff14ipq, ff15ipq, and fb15, which were not designed to be compatible with GB models, were consistently poor at maintaining the peptide's starting conformation (median α helicity < 50%) regardless of the GB model, Figures 1b and S2.

The simulations were sensitive to both the GB model and to the force field used: different predominant secondary structures were predicted by the same force field when different GB models were used and vice versa. Some force fields, e.g., ff96, ff03.r1, and ff14SB, were much more sensitive

https://doi.org/10.1021/acs.jctc.1c01172
J. Chem. Theory Comput. 2022, 18, 4070−4076

to the choice of the implicit solvent model, with some GB models giving a median helicity above 70% and others below 50%. For example, ff96 with igb5 captured the α helicity relatively well (median helicity ≈ 83%), but the same force field with igb8 predicted formation of a β hairpin (within 1 μs) which developed into a stable three-stranded sheet over the remainder of the simulation. In contrast, these force fields with igb7, the $A_4(K_4E_4)_1A_4(K_4E_4)_1A_4$ showed the peptide as disordered (Figures 1b and S1 and Movie S2).

To test the reproducibility of these simulations, we ran a total of four replicas for each of several GB model−force field combinations (Figures S3 and S4). These repeated simulations gave similar structures, and the differences between replicas are, in most cases, minimal. Reassuringly, the same major conformational changes were sampled in all four replica runs, albeit at different times, e.g., the α helix-to-β structure transitions observed with the igb8−ff96 combination. These results indicate that a single 6 μs simulation sufficiently captures the performance of a GB model−force field combination for peptides of this size, but replica simulations should be run to ensure the reproducibility of the results for the best performing combinations.

Although none of the GB model−force field combinations maintained the experimentally observed helicity of $A_4(K_4E_4)_1A_4(K_4E_4)_1A_4$, several gave a high degree of helicity (median helicity > 75%). Therefore, we tested these combinations, along with some others for comparison, on other peptides with lower experimental α-helical content, i.e., the pair $(E_4K_4)_2$ (65% α helix) and $(K_4E_4)_2$ (22% α helix), Table 1, which differ only in the order of the Glu_4 and Lys_4 blocks. For these peptides, 27 implicit solvent−force field combinations were tested, starting from fully α-helical conformations of both peptides and using the same protocols as for $A_4(K_4E_4)_1A_4(K_4E_4)_1A_4$. We note that a peptide similar to $(E_4K_4)_2$, differing only in the absence of Gly and of Gly and Trp residues at the *N* and *C* termini, respectively, has been studied by replica-exchange MD (REMD) in explicit TIP3P water using the ff03.r1 force field,[16] which reproduced the experimentally determined helicity of the peptide at different temperatures with good accuracy.

In our simulations, the older force fields (ff94, ff96, ff98, and ff99SBnmr), which captured the high α-helical content of $A_4(K_4E_4)_1A_4(K_4E_4)_1A_4$, consistently predicted high α helicities for both $(E_4K_4)_2$ and $(K_4E_4)_2$, Figure 2a. They did not discriminate between $(E_4K_4)_2$ and $(K_4E_4)_2$, regardless of the GB model, with median helicities for both peptides of ≈80% versus experimental values of 67% and 22%, respectively. These force fields appear to systematically favor and overestimate the α-helical structure, at least for these Glu/Lys-rich peptides. In contrast, the more recent force fields ff03.r1 and ff14SB gave lower α helicities that were closer to the experimentally determined values (except in the case of ff03.r1 with igb8), Figure 2a. Moreover, they correctly predicted $(E_4K_4)_2$ to be more helical than $(K_4E_4)_2$, although the differences in predicted helicities between the two peptides were less than measured experimentally. ff14SB performed better than ff03.r1. The combination of ff14SB with igb7, which failed to predict the experimentally determined α helicity of $A_4(K_4E_4)_1A_4(K_4E_4)_1A_4$ (13% vs 97%) (Figure 1), gave the best prediction of the difference in helicity between $(E_4K_4)_2$ and $(K_4E_4)_2$ (63% and 21%, respectively). Overall, our results reveal that even when a particular GB model−force field combination describes a particular peptide well, it may fail for a closely related homologue, for instance, one with the same composition but a different order of the amino acid residues.

To test this last point further, we took the eight GB model−force field combinations that performed best for $(E_4K_4)_2$ and $(K_4E_4)_2$ and modeled their longer counterparts, namely $(E_4K_4)_3$ and $(K_4E_4)_3$, Table 1, which have a smaller difference in experimental α helicities, i.e., 74% and 62%, respectively. Again, the different methods predicted a wide range of helicities (Figure 2b). Both ff03.r1 with igb5 and ff14SB with igb7 gave results in reasonable agreement with the experimental helicity for the two peptides, with median α helicities of 67% and 78%, respectively, for $(E_4K_4)_3$ and 59% and 56%, respectively, for $(K_4E_4)_3$. ff14SB with igb1 and igb5 also correctly predicted $(E_4K_4)_3$ as the more helical peptide, although the median helicities were 10% to 20% lower than experiment.

Overall, the combination of ff14SB with igb7 stood out, having predicted the percentage helicities for $(E_4K_4)_2$, $(K_4E_4)_2$, $(E_4K_4)_3$, and $(K_4E_4)_3$ reasonably well; i.e., all were within 10% of the experimental values (Figure 2). However, it failed to predict the high helicity of $A_4(K_4E_4)_1A_4(K_4E_4)_1A_4$, Figure 1a, returning random conformations instead (Figure 1b). Moreover, the combinations that best predicted the helicity of $A_4(K_4E_4)_1A_4(K_4E_4)_1A_4$ did not replicate the percentage helicities for the other four peptides and almost always failed to predict the more helical of the paired designs. Thus, none of the GB−force field combinations tested here are a reliable predictor for all five of the peptides that we tested.

To test these findings further, we performed further analysis of the original experimental CD data using a different method, BeStSel[24,44] (see Supplementary Results), which fits CD spectra to linear combinations of components derived from DSSP. Fitting of the experimental CD data was performed using the BeStSel Web server[24] for the 200−250 nm region. BeStSel gave some differences in values of α helicity from those originally reported;[15] in particular for $A_4(K_4E_4)_1A_4(K_4E_4)_1A_4$, which was calculated to be 77% α helical using BeStSel vs 97% originally (Table 1). However, the results obtained from using BeStSel-predicted helicities did not change our conclusions: none of the GB model−force field combinations were predictive for all five peptides, and none were able to correctly model the fraction of other secondary structures identified by BeStSel.

Several important factors should be noted. REMD[45] was not used here,because the goal was to look at a fast approach that can be applied in protein design. REMD might improve convergence but is not likely to change the overall conclusion that the GB models are not predictive of secondary structures adopted by these peptides: as shown above, conformational sampling of these peptides on these time scales under these conditions appears reasonable for these purposes. Similarly, the surface area (SA) term, which approximates nonpolar contributions to the solvation free energy, was not computed because the goal was to test fast approaches useful to nonexperts (i.e., using default options), and at the time the simulations were conducted, GBSA simulations could not be run on GPUs with AMBER. Although approximating nonpolar solvation using solvent accessible surface area has limitations,[46,47] repeating the simulations using GBSA would be interesting. However, it is unlikely to change the results drastically as the electrostatic term is expected to be dominant for these peptides. Neglecting nonpolar terms has been shown to perform well for small peptides.[14,29] Also, all the Glu and

https://doi.org/10.1021/acs.jctc.1c01172
J. Chem. Theory Comput. 2022, 18, 4070−4076

Lys residues were treated as ionized. Interactions between such charged residues can lead to changes in effective pK_a (coupled pK_as) and hence in the protonation state.[48] Using constant pH, MD[49,50] could shed further light on this and on any effect on the secondary structure. Finally, it would be interesting to explore combinations of force fields with explicit solvent models on the same Glu- and Lys-rich peptides.

In summary, none of the GB model−force field combinations that we have tested accurately reproduce the experimentally measured α helicities of the five peptides. While some GB model−force field combinations systematically show a high degree of helicity, irrespective of the peptide, others are only predictive for peptides with high or intermediate α helicities. Furthermore, some combinations predict entirely incorrect conformations, including β-rich or disordered structures, for which there is no experimental evidence. Therefore, our simulations serve as a warning of the potential unreliability of GB models for some predictions of protein/peptide properties and a reminder of the importance of the force field: for the peptides studied here, changing the force field for a given GB model usually leads to changes that are more marked than changing the GB model for a given force field. They also highlight the importance, whenever possible, of rigorously testing GB models and force fields against experimental data.

Explicit solvent simulations give good results for similar peptides.[16,20−22] The recommendation to the protein designer currently would therefore be to use explicit solvent MD simulations. Inclusion of nonelectrostatic solvation terms may improve results and would be recommended for protein design applications with implicit solvent models. The small peptides here may not be representative of the behavior of larger, folded proteins, and implicit solvent simulations may well be useful for refining such structures, which are likely to remain folded on reasonable time scales. We also acknowledge the limited sequence variation of the highly repetitive peptides modeled, as well as their relatively unusual charge distributions, which may make them particularly challenging to model. However, similar features are found in naturally occurring proteins.[16−19] These *de novo* peptides provide a useful training set for simulations and machine learning and for testing solvent models and protein force fields.

■ ASSOCIATED CONTENT

Supporting Information

The Supporting Information is available free of charge at https://pubs.acs.org/doi/10.1021/acs.jctc.1c01172.

Methods; supplementary results; Figure S1, percentage α helicity of $A_4(K_4E_4)_1A_4(K_4E_4)_1A_4$ as function of simulation time; Figure S2, average secondary structures; Figure S3, predicted α helicity from replica MD simulations; Figure S4, α helicity as function of time from replica MD simulations; Figure S5, percentage α helicity of $(E_4K_4)_2$ and $(K_4E_4)_2$ peptides; Figure S6, percentage helicity of $(E_4K_4)_3$ and $(K_4E_4)_3$ peptides; Figures S7−S11, results of BeStSel fitting of experimental CD curve for $A_4(K_4E_4)_1A_4(K_4E_4)_1A_4$, $(E_4K_4)_2$, $(K_4E_4)_2$, $(E_4K_4)_3$, and $(K_4E_4)_3$, respectively; and Table S1, fraction helicity calculated from experimental CD data using BeStSel (PDF)

Movie S1, trajectories of 6 μs MD simulations of $A_4(K_4E_4)_1A_4(K_4E_4)_1A_4$ using igb5 (MP4)

Movie S2, trajectories of 6 μs MD simulations of $A_4(K_4E_4)_1A_4(K_4E_4)_1A_4$ using ff96 (MP4)

■ AUTHOR INFORMATION

Corresponding Authors

Adrian J. Mulholland − *Centre for Computational Chemistry, School of Chemistry, University of Bristol, Bristol BS8 1TS, U.K.; School of Chemistry, University of Bristol, Bristol BS8 1TS, U.K.;* orcid.org/0000-0003-1015-4567; Email: adrian.mulholland@bristol.ac.uk

Eric J. M. Lang − *Centre for Computational Chemistry, School of Chemistry, University of Bristol, Bristol BS8 1TS, U.K.; School of Chemistry, University of Bristol, Bristol BS8 1TS, U.K.; BrisSynBio, University of Bristol, Bristol BS8 1TQ, U.K.;* Email: eric.jm.lang@gmail.com

Authors

Emily G. Baker − *School of Chemistry, University of Bristol, Bristol BS8 1TS, U.K.; BrisSynBio, University of Bristol, Bristol BS8 1TQ, U.K.;* orcid.org/0000-0002-1593-5525

Derek N. Woolfson − *School of Chemistry, University of Bristol, Bristol BS8 1TS, U.K.; BrisSynBio, University of Bristol, Bristol BS8 1TQ, U.K.; School of Biochemistry, University of Bristol, Bristol BS8 1TD, U.K.;* orcid.org/0000-0002-0394-3202

Complete contact information is available at: https://pubs.acs.org/10.1021/acs.jctc.1c01172

Author Contributions

E.J.M.L. conceived the project. E.J.M.L., D.N.W., and A.J.M. designed the research. E.J.M.L. performed the research. E.J.M.L analyzed the data with contributions from all authors. E.G.B. collected the experimental CD data. All the authors contributed to writing the manuscript. All authors have given approval to the final version of the manuscript.

Notes

The authors declare no competing financial interest.

Data access statement: All structures, scripts and data used in this study are available at https://github.com/eric-jm-lang/GB_simulations_de_novo_peptides.

■ ACKNOWLEDGMENTS

E.J.M.L., A.J.M., and D.N.W. were funded by the BBSRC/EPSRC Synthetic Biology Research Centre, BrisSynBio (BB/L01386X/1). A.J.M. also thanks the EPSRC for support (EP/M022609/1). D.N.W. held a Royal Society Wolfson Research Merit Award (WM140008). The authors thank Robert E. Arbon for help with the statistical analysis of the MD data. This work was carried out using the computational facilities (BlueCrystal Phase 4) of the Advanced Computing Research Centre, University of Bristol (http://www.bris.ac.uk/acrc/). We thank Prof. Thomas Simonson for useful discussions.

■ ABBREVIATIONS

GB, generalized Born; MD, molecular dynamics; CD, circular dichroism; REMD, replica exchange molecular dynamics

■ REFERENCES

(1) Huggins, D. J.; Biggin, P. C.; Dämgen, M. A.; Essex, J. W.; Harris, S. A.; Henchman, R. H.; Khalid, S.; Kuzmanic, A.; Laughton, C. A.; Michel, J.; Mulholland, A. J.; Rosta, E.; Sansom, M. S. P.; van der Kamp, M. W. Biomolecular Simulations: From Dynamics and

Mechanisms to Computational Assays of Biological Activity. *WIREs Comput. Mol. Sci.* **2019**, *9* (3), No. e1393.
(2) Park, H.; DiMaio, F.; Baker, D. The Origin of Consistent Protein Structure Refinement from Structural Averaging. *Structure* **2015**, *23* (6), 1123−1128.
(3) Park, H.; Lee, G. R.; Kim, D. E.; Anishchenko, I.; Cong, Q.; Baker, D. High-Accuracy Refinement Using Rosetta in CASP13. *Proteins Struct. Funct. Bioinforma.* **2019**, *87* (12), 1276−1282.
(4) Crean, R. M.; Gardner, J. M.; Kamerlin, S. C. L. Harnessing Conformational Plasticity to Generate Designer Enzymes. *J. Am. Chem. Soc.* **2020**, *142* (26), 11324−11342.
(5) Bunzel, H. A.; Anderson, J. L. R.; Mulholland, A. J. Designing Better Enzymes: Insights from Directed Evolution. *Curr. Opin. Struct. Biol.* **2021**, *67*, 212−218.
(6) Ge, Y.; Kier, B. L.; Andersen, N. H.; Voelz, V. A. Computational and Experimental Evaluation of Designed β-Cap Hairpins Using Molecular Simulations and Kinetic Network Models. *J. Chem. Inf. Model.* **2017**, *57* (7), 1609−1620.
(7) Onufriev, A. V.; Case, D. A. Generalized Born Implicit Solvent Models for Biomolecules. *Annu. Rev. Biophys.* **2019**, *48* (1), 275−296.
(8) Kleinjung, J.; Fraternali, F. Design and Application of Implicit Solvent Models in Biomolecular Simulations. *Curr. Opin. Struct. Biol.* **2014**, *25*, 126−134.
(9) Zagrovic, B.; Pande, V. Solvent Viscosity Dependence of the Folding Rate of a Small Protein: Distributed Computing Study. *J. Comput. Chem.* **2003**, *24* (12), 1432−1436.
(10) Anandakrishnan, R.; Drozdetski, A.; Walker, R. C.; Onufriev, A. V. Speed of Conformational Change: Comparing Explicit and Implicit Solvent Molecular Dynamics Simulations. *Biophys. J.* **2015**, *108* (5), 1153−1164.
(11) Shell, M. S.; Ritterson, R.; Dill, K. A. A Test on Peptide Stability of AMBER Force Fields with Implicit Solvation. *J. Phys. Chem. B* **2008**, *112* (22), 6878−6886.
(12) Robinson, M. K.; Monroe, J. I.; Shell, M. S. Are AMBER Force Fields and Implicit Solvation Models Additive? A Folding Study with a Balanced Peptide Test Set. *J. Chem. Theory Comput.* **2016**, *12* (11), 5631−5642.
(13) Maffucci, I.; Contini, A. An Updated Test of AMBER Force Fields and Implicit Solvent Models in Predicting the Secondary Structure of Helical, β-Hairpin, and Intrinsically Disordered Peptides. *J. Chem. Theory Comput.* **2016**, *12* (2), 714−727.
(14) Nguyen, H.; Maier, J.; Huang, H.; Perrone, V.; Simmerling, C. Folding Simulations for Proteins with Diverse Topologies Are Accessible in Days with a Physics-Based Force Field and Implicit Solvent. *J. Am. Chem. Soc.* **2014**, *136* (40), 13959−13962.
(15) Baker, E. G.; Bartlett, G. J.; Crump, M. P.; Sessions, R. B.; Linden, N.; Faul, C. F. J.; Woolfson, D. N. Local and Macroscopic Electrostatic Interactions in Single α-Helices. *Nat. Chem. Biol.* **2015**, *11* (3), 221−228.
(16) Sivaramakrishnan, S.; Spink, B. J.; Sim, A. Y. L.; Doniach, S.; Spudich, J. A. Dynamic Charge Interactions Create Surprising Rigidity in the ER/K α-Helical Protein Motif. *Proc. Natl. Acad. Sci. U. S. A.* **2008**, *105* (36), 13356−13361.
(17) Swanson, C. J.; Sivaramakrishnan, S. Harnessing the Unique Structural Properties of Isolated α-Helices *. *J. Biol. Chem.* **2014**, *289* (37), 25460−25467.
(18) Gáspári, Z.; Süveges, D.; Perczel, A.; Nyitray, L.; Tóth, G. Charged Single Alpha-Helices in Proteomes Revealed by a Consensus Prediction Approach. *Biochim. Biophys. Acta BBA - Proteins Proteomics* **2012**, *1824* (4), 637−646.
(19) Peckham, M.; Knight, P. J. When a Predicted Coiled Coil Is Really a Single α-Helix, in Myosins and Other Proteins. *Soft Matter* **2009**, *5* (13), 2493−2503.
(20) Wolny, M.; Batchelor, M.; Bartlett, G. J.; Baker, E. G.; Kurzawa, M.; Knight, P. J.; Dougan, L.; Woolfson, D. N.; Paci, E.; Peckham, M. Characterization of Long and Stable de Novo Single Alpha-Helix Domains Provides Novel Insight into Their Stability. *Sci. Rep.* **2017**, *7* (1), 44341.
(21) Batchelor, M.; Wolny, M.; Baker, E. G.; Paci, E.; Kalverda, A. P.; Peckham, M. Dynamic Ion Pair Behavior Stabilizes Single α-Helices in Proteins. *J. Biol. Chem.* **2019**, *294* (9), 3219−3234.
(22) Collu, G.; Bierig, T.; Krebs, A.-S.; Engilberge, S.; Varma, N.; Guixà-González, R.; Sharpe, T.; Deupi, X.; Olieric, V.; Poghosyan, E.; Benoit, R. M. Chimeric Single α-Helical Domains as Rigid Fusion Protein Connections for Protein Nanotechnology and Structural Biology. *Structure* **2022**, *30* (1), 95−106.e7.
(23) Case, D. A.; Walker, R. C.; Cheatham, T. E.; Simmerling, C.; Roitberg, A. E.; Merz, K. M.; Luo, R.; Darden, T.; Wang, J.; Duke, R. E.; Le Grand, S.; Swails, J. M.; Cerutti, D. S.; Monard, G.; Sagui, C.; Kaus, J.; Betz, R.; Madej, B.; Lin, C.; Mermelstein, D.; Li, P.; Onufriev, A. V.; Izadi, S.; Wolf, R. M.; Wu, X.; Götz, A. W.; Gohlke, H.; Homeyer, N.; Botello-Smith, W. M.; Xiao, L.; Luchko, T.; Giese, T.; Lee, T.; Nguyen, H. T.; Nguyen, H.; Janowski, P.; Omelyan, I.; Kovalenko, A.; Kollman, P. A. *Amber 2016*; 2016.
(24) Micsonai, A.; Wien, F.; Bulyáki, É.; Kun, J.; Moussong, É.; Lee, Y.-H.; Goto, Y.; Réfrégiers, M.; Kardos, J. BeStSel: A Web Server for Accurate Protein Secondary Structure Prediction and Fold Recognition from the Circular Dichroism Spectra. *Nucleic Acids Res.* **2018**, *46* (W1), W315−W322.
(25) Hawkins, G. D.; Cramer, C. J.; Truhlar, D. G. Pairwise Solute Descreening of Solute Charges from a Dielectric Medium. *Chem. Phys. Lett.* **1995**, *246* (1), 122−129.
(26) Onufriev, A.; Bashford, D.; Case, D. A. Modification of the Generalized Born Model Suitable for Macromolecules. *J. Phys. Chem. B* **2000**, *104* (15), 3712−3720.
(27) Onufriev, A.; Bashford, D.; Case, D. A. Exploring Protein Native States and Large-Scale Conformational Changes with a Modified Generalized Born Model. *Proteins Struct. Funct. Bioinforma.* **2004**, *55* (2), 383−394.
(28) Mongan, J.; Simmerling, C.; McCammon, J. A.; Case, D. A.; Onufriev, A. Generalized Born Model with a Simple, Robust Molecular Volume Correction. *J. Chem. Theory Comput.* **2007**, *3* (1), 156−169.
(29) Nguyen, H.; Roe, D. R.; Simmerling, C. Improved Generalized Born Solvent Model Parameters for Protein Simulations. *J. Chem. Theory Comput.* **2013**, *9* (4), 2020−2034.
(30) Cornell, W. D.; Cieplak, P.; Bayly, C. I.; Gould, I. R.; Merz, K. M.; Ferguson, D. M.; Spellmeyer, D. C.; Fox, T.; Caldwell, J. W.; Kollman, P. A. A Second Generation Force Field for the Simulation of Proteins, Nucleic Acids, and Organic Molecules. *J. Am. Chem. Soc.* **1995**, *117* (19), 5179−5197.
(31) Kollman, P.; Dixon, R.; Cornell, W.; Fox, T.; Chipot, C.; Pohorille, A. The Development/Application of a 'Minimalist' Organic/Biochemical Molecular Mechanic Force Field Using a Combination of Ab Initio Calculations and Experimental Data. In *Computer Simulation of Biomolecular Systems: Theoretical and Experimental Applications*; van Gunsteren, W. F., Weiner, P. K., Wilkinson, A. J., Eds.; Computer Simulations of Biomolecular Systems; Springer Netherlands: Dordrecht, 1997; pp 83−96, DOI: 10.1007/978-94-017-1120-3_2.
(32) Cheatham, T. E., III; Cieplak, P.; Kollman, P. A. A Modified Version of the Cornell et al. Force Field with Improved Sugar Pucker Phases and Helical Repeat. *J. Biomol. Struct. Dyn.* **1999**, *16* (4), 845−862.
(33) Wang, J.; Cieplak, P.; Kollman, P. A. How well does a restrained electrostatic potential (RESP) model perform in calculating conformational energies of organic and biological molecules? *J. Comput. Chem.* **2000**, *21* (12), 1049−1074.
(34) Hornak, V.; Abel, R.; Okur, A.; Strockbine, B.; Roitberg, A.; Simmerling, C. Comparison of Multiple Amber Force Fields and Development of Improved Protein Backbone Parameters. *Proteins Struct. Funct. Bioinforma.* **2006**, *65* (3), 712−725.
(35) Lindorff-Larsen, K.; Piana, S.; Palmo, K.; Maragakis, P.; Klepeis, J. L.; Dror, R. O.; Shaw, D. E. Improved Side-Chain Torsion Potentials for the Amber Ff99SB Protein Force Field. *Proteins Struct. Funct. Bioinforma.* **2010**, *78* (8), 1950−1958.

(36) Li, D.-W.; Brüschweiler, R. NMR-Based Protein Potentials. *Angew. Chem., Int. Ed.* **2010**, *49* (38), 6778−6780.
(37) Duan, Y.; Wu, C.; Chowdhury, S.; Lee, M. C.; Xiong, G.; Zhang, W.; Yang, R.; Cieplak, P.; Luo, R.; Lee, T.; Caldwell, J.; Wang, J.; Kollman, P. A point-charge force field for molecular mechanics simulations of proteins based on condensed-phase quantum mechanical calculations. *J. Comput. Chem.* **2003**, *24* (16), 1999−2012.
(38) Maier, J. A.; Martinez, C.; Kasavajhala, K.; Wickstrom, L.; Hauser, K. E.; Simmerling, C. Ff14SB: Improving the Accuracy of Protein Side Chain and Backbone Parameters from Ff99SB. *J. Chem. Theory Comput.* **2015**, *11* (8), 3696−3713.
(39) Cerutti, D. S.; Swope, W. C.; Rice, J. E.; Case, D. A. Ff14ipq: A Self-Consistent Force Field for Condensed-Phase Simulations of Proteins. *J. Chem. Theory Comput.* **2014**, *10* (10), 4515−4534.
(40) Wang, L.-P.; McKiernan, K. A.; Gomes, J.; Beauchamp, K. A.; Head-Gordon, T.; Rice, J. E.; Swope, W. C.; Martínez, T. J.; Pande, V. S. Building a More Predictive Protein Force Field: A Systematic and Reproducible Route to AMBER-FB15. *J. Phys. Chem. B* **2017**, *121* (16), 4023−4039.
(41) Debiec, K. T.; Cerutti, D. S.; Baker, L. R.; Gronenborn, A. M.; Case, D. A.; Chong, L. T. Further along the Road Less Traveled: AMBER Ff15ipq, an Original Protein Force Field Built on a Self-Consistent Physical Model. *J. Chem. Theory Comput.* **2016**, *12* (8), 3926−3947.
(42) Götz, A. W.; Williamson, M. J.; Xu, D.; Poole, D.; Le Grand, S.; Walker, R. C. Routine Microsecond Molecular Dynamics Simulations with AMBER on GPUs. 1. Generalized Born. *J. Chem. Theory Comput.* **2012**, *8* (5), 1542−1555.
(43) Kabsch, W.; Sander, C. Dictionary of Protein Secondary Structure: Pattern Recognition of Hydrogen-Bonded and Geometrical Features. *Biopolymers* **1983**, *22* (12), 2577−2637.
(44) Micsonai, A.; Wien, F.; Kernya, L.; Lee, Y.-H.; Goto, Y.; Réfrégiers, M.; Kardos, J. Accurate Secondary Structure Prediction and Fold Recognition for Circular Dichroism Spectroscopy. *Proc. Natl. Acad. Sci. U. S. A.* **2015**, *112* (24), No. E3095-E3103.
(45) Sugita, Y.; Okamoto, Y. Replica-Exchange Molecular Dynamics Method for Protein Folding. *Chem. Phys. Lett.* **1999**, *314* (1), 141−151.
(46) Levy, R. M.; Zhang, L. Y.; Gallicchio, E.; Felts, A. K. On the Nonpolar Hydration Free Energy of Proteins: Surface Area and Continuum Solvent Models for the Solute-Solvent Interaction Energy. *J. Am. Chem. Soc.* **2003**, *125* (31), 9523−9530.
(47) Chen, J.; Brooks, C. L., III Implicit Modeling of Nonpolar Solvation for Simulating Protein Folding and Conformational Transitions. *Phys. Chem. Chem. Phys.* **2008**, *10* (4), 471−481.
(48) Rhys, G. G.; Wood, C. W.; Lang, E. J. M.; Mulholland, A. J.; Brady, R. L.; Thomson, A. R.; Woolfson, D. N. Maintaining and Breaking Symmetry in Homomeric Coiled-Coil Assemblies. *Nat. Commun.* **2018**, *9* (1), 4132.
(49) Mongan, J.; Case, D. A.; McCammon, J. A. Constant PH Molecular Dynamics in Generalized Born Implicit Solvent. *J. Comput. Chem.* **2004**, *25* (16), 2038−2048.
(50) Swails, J. M.; Roitberg, A. E. Enhancing Conformation and Protonation State Sampling of Hen Egg White Lysozyme Using PH Replica Exchange Molecular Dynamics. *J. Chem. Theory Comput.* **2012**, *8* (11), 4393−4404.

https://doi.org/10.1021/acs.jctc.1c01172
J. Chem. Theory Comput. 2022, 18, 4070−4076